

# Quantum-dot-free Two-step Photon Up-conversion Solar Cells based on Cesium Lead Bromide/Gallium Arsenide Interface

Hambalee Mahamu, Shigeo Asahi, and Takashi Kita

*Department of Electrical and Electronics Engineering, Graduate School of Engineering,  
Kobe University*

Two-step photon up-conversion (TPU) is a physical phenomenon that allows below-bandgap photon absorption caused by quantized states at a heterointerface which relaxes optical selection rules. In this work, we study the TPU process in a quantum-dot-free simple structure of cesium lead bromide/GaAs-based solar cells (SCs). The enhancement of photocurrent was comprehensively studied by measuring the below-bandgap photoexcitation power dependence of the gained photocurrent to figure out the characteristics of the TPU of the SCs. Although the photocurrent can be enhanced by below-bandgap photoirradiation, the improvement depends on the interband excitation power. The absorptivity of 1319-nm photon, the below-bandgap photons we used, shows that the possibility of the photocurrent enhancement is likely to be due to the interface states because of the very small absorption coefficient compared to the one for quantum dots.

## 1. Introduction

Two-step photon up-conversion solar cells (TPU-SCs), on the other hand, were proposed to suppress the problems of the IBSCs [1, 2]. The TPU-SCs consist of two main absorbers. One absorber exhibits a wider bandgap, called a wide-gap semiconductor (WGS), and the other is a narrow-gap semiconductor (NGS). A layer of quantum dots (QDs) was inserted into the heterointerface to create quantized states aiming to relax the optical selection rules and allow the in-plane electronic transitions. The experimentally achieved TPU-SCs were based on III-V semiconductors, namely  $\text{Al}_{0.3}\text{Ga}_{0.7}\text{As}$  (as the WGS) and GaAs (as the NGS) with InAs QDs grown at the heterointerface. By this structure, the photocurrent was enhanced together with photovoltage. The fabrication technique is relatively easier compared to the IBSCs since the TPU-SCs do not need the IB, and hence, a single layer of QDs is satisfactory.

In this work, we created a quantum-dot-free simple TPU-SC based on the utilization of

cesium lead bromide ( $\text{CsPbBr}_3$ ) perovskite acting as a WGS and GaAs acting as an NGS. Because perovskites exhibit polycrystalline in general, we expect that the interface states, which are considered to be ‘defects’, can behave like quantized states in the TPU-SCs. Therefore, the enhancement of the photocurrent is expected to be observed.

## 2. Fabrication of Solar Cells

We proposed a simple *n-i-p* structure of SCs as indicated in Fig. 1(a). We used *p*-GaAs substrates (001) for NGS. The surface of the substrates was cleaned in acetone, methanol, isopropanol, and deionized water respectively before they were used. For  $\text{CsPbBr}_3$  WGS, we synthesized two solutions of  $\text{CsPbBr}_3$  precursors including 1 M of lead (II) bromide ( $\text{PbBr}_2$ ) in dimethylformamide (DMF) and 0.07 M of cesium bromide (CsBr) in 5:1 methanol and water mixture. The solutions were stirred at 90 °C for 30 minutes. Next, the solutions were filtered by microporous filters to avoid microcrystals and turbidity.

Subsequently, several drops of  $\text{PbBr}_2$  were dropped on a p-GaAs substrate. The substrate was spun at 2000 rpm for 30 seconds. After the first 5 seconds, 100  $\mu\text{L}$  of chlorobenzene was dropped on the spinning substrate for the antisolvent method. Next, the substrate was heated on a hotplate immediately at 90  $^\circ\text{C}$  for 30 minutes. The  $\text{PbBr}_2$  contained p-GaAs substrate was, next, installed in the spin coater. Several drops of CsBr solution were dropped on the substrate. Then, the substrate was spun at the same spin conditions before it was immediately heated at 250  $^\circ\text{C}$  for 5 minutes. This process was repeated 4 times in order to achieve high purity of  $\text{CsPbBr}_3$  perovskite phase. The band diagram of the SCs, calculated by COMSOL Multiphysics®, is indicated in Fig. 1(b).

### 3. Results and Discussions

We measured the photoluminescence (PL) and the external quantum efficiency (EQE) spectra (Fig. 2) without an additional 1319-nm infrared photoirradiation. Figure 2(a) shows the PL spectrum of  $\text{CsPbBr}_3$  where the peak is at  $\sim 530$  nm. A small peak attributed to GaAs also appears slightly at  $\sim 870$  nm. The PL result is consistent with the EQE spectrum shown in Fig. 2(b). The absorption edges of  $\text{CsPbBr}_3$  and GaAs are seen at  $\sim 530$  nm and  $\sim 870$  nm respectively.

Furthermore, we measured 784-nm interband excitation and 1319-nm intraband excitation power dependence of the gained photocurrent defined as  $\Delta J_{\text{sc}} = J_{\text{sc, with infrared}} - J_{\text{sc, without infrared}}$ . The increase in interband excitation intensity means the increasing electron injection rate to the interface meanwhile the increase in interband excitation intensity corresponds to the electron escapes from the interface. Therefore, linear relationship of 784-nm interband excitation to the electron density at

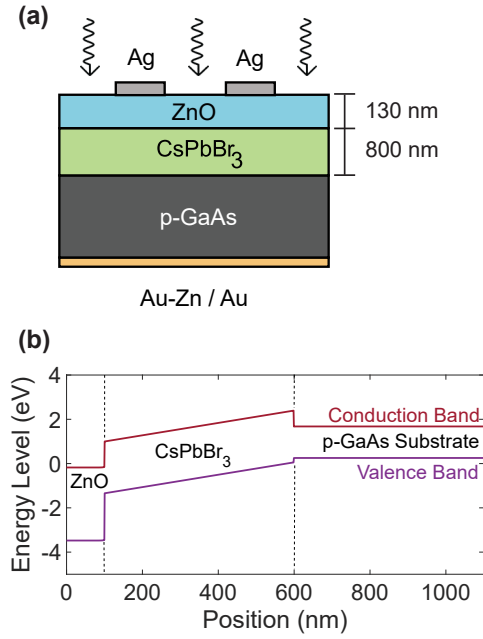


Fig.1 Schematic structure of  $\text{CsPbBr}_3/\text{GaAs}$ -based TPU-SCs and their band diagram.

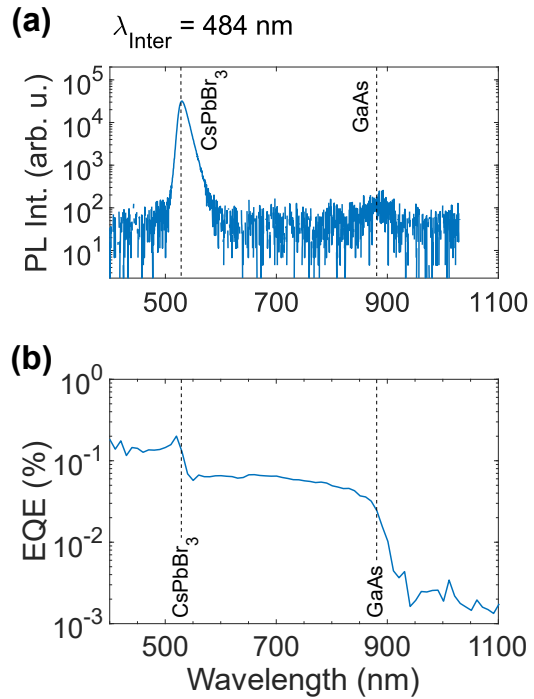


Fig.2 (a) Photoluminescence spectrum of  $\text{CsPbBr}_3$ . (b) External quantum efficiency of  $\text{CsPbBr}_3/\text{GaAs}$ -based TPU-SCs.

the interface is expected if there is no loss during the electron injection. Moreover, we measured the  $\Delta J_{\text{sc}}$  which is influenced by the intraband excitation, thermal activation, and losses during the electron transport process. As a result, the  $\Delta J_{\text{sc}}$  is inequivalent to the electron density at the

interface providing the estimated power index,  $n = 0.88$  as shown in Fig. 3(a). This points out that there is loss of photogenerated electrons which is likely to be due to the recombination at the interface. Considering, 784-nm photons excite GaAs generating electrons in the CB and holes in the VB. The electrons drift toward the interface in contrast to holes that drift toward the bottom electrodes. The recombination at the CsPbBr<sub>3</sub>/GaAs interface is possible due to hole diffusion to the interface causing the reduction of electron density. This phenomenon was reported elsewhere [3]. Meanwhile, the hole density at the ZnO/ CsPbBr<sub>3</sub> interface plays insignificant roles since there is no photogenerated holes in CsPbBr<sub>3</sub> layer. Hence, the hole density at the ZnO/ CsPbBr<sub>3</sub> interface is contributed by the up-converted diffusing holes from the CsPbBr<sub>3</sub> /GaAs interface which is hardly to occur.

The  $\Delta J_{sc}$  data as a function of 1319-nm intraband excitation power density is visualized

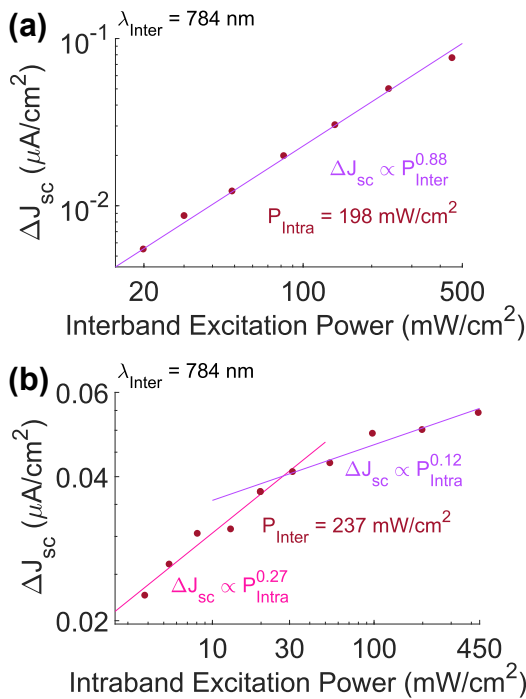


Fig.3 (a) Gained photocurrent as a function of 784-nm interband excitation power density. (b) Gained photocurrent as a function of 1319-nm intraband excitation power density.

in Fig. 3(b). The data cannot be fitted by a single power function, which means the carrier dynamics depend on the carrier density. Such an identical characteristic was reported in our previous publication on the doubled-heterointerface TPU-SCs [3]. The characteristics shown in Fig. 3(b) can be divided into two features. The first one is where the intraband excitation power density is small. Here, the estimated power index is 0.27. The power index changes where the intraband excitation power density is about  $20 \text{ mW}/\text{cm}^2$ . The power index, here at the second feature, reduces from 0.27 to 0.12 which is about half of the original one. Because a reduced power index is a decrease in photoresponsivity and we, in addition, observed the TPU process at the ZnO/ CsPbBr<sub>3</sub> interface, the reduction of the power index can be interpreted as malfunction of either the CsPbBr<sub>3</sub> /GaAs interface or the ZnO/ CsPbBr<sub>3</sub> interface.

Considering the mechanisms, we need to state here, firstly, that the recombination at the CsPbBr<sub>3</sub> /GaAs interface cannot play an important role in the reduction of the power index. That is because of the diffusing hole density at the interface only depends on 784-nm interband excitation intensity which was fixed at  $237 \text{ mW}/\text{cm}^2$ . The recombination at the ZnO/ CsPbBr<sub>3</sub> interface is not significant as aforementioned. The change in the power index, therefore, is only caused by the change in electron density at the two interfaces. Secondly, the interface states are well-known for their weak density of states. At low intraband excitation intensity, the electron density at the ZnO/ CsPbBr<sub>3</sub> interface is supplied by intraband-excited electrons from the CsPbBr<sub>3</sub> /GaAs interface. In this case, the intraband-excited electrons at both interfaces can contribute to the  $\Delta J_{sc}$  data. When the

intraband excitation increases, the interface states at the ZnO/CsPbBr<sub>3</sub> interface can be relatively easier filled with electrons compared to those at the CsPbBr<sub>3</sub>/GaAs interface due to the possibility of recombination with the diffusing holes. Such a state-filling-like phenomenon at the ZnO/CsPbBr<sub>3</sub> interface limits the intraband-excited electrons from the CsPbBr<sub>3</sub>/GaAs interface to be collected as photocurrent. Consequently, the estimated power index or the photoresponsivity reduces as indicated in Fig. 3(b).

The absorptivity of 1319-nm infrared photons was calculated using the equation shown as follows:

$$\Delta J_{sc} = qN_{in} A \quad (1)$$

where  $\Delta J_{sc}$  is gained photocurrent,  $q$  is the elementary charge,  $N_{in}$  is incident 1319-nm infrared photons flux, and  $A$  is the absorptivity. The obtained absorptivity map (Fig. 4) reveals that the absorptivity decreases with an increase in intraband excitation power density meanwhile it increases with interband excitation power density. The reducing absorptivity with increasing intraband excitation intensity is due to the reduction of electron density at the interface. As a result, the highest absorptivity of 1319-nm infrared photon can be seen at high interband excitation intensity but low intraband excitation intensity.

We compared the absorption coefficient calculated from the modified Eq. 1 shown as follows:

$$\alpha = -\frac{1}{x} \ln \left( 1 - \frac{\Delta J_{sc}}{qN_{in}} \right) \quad (2)$$

where  $\alpha$  is the absorption coefficient and  $x$  is the thickness of electron density accumulating at the interface. This thickness was assumed to be 3 nm, which is the same as that for fabricated InAs QDs in our laboratory [2, 3]. Because the TPU is a nonlinear phenomenon, the absorption

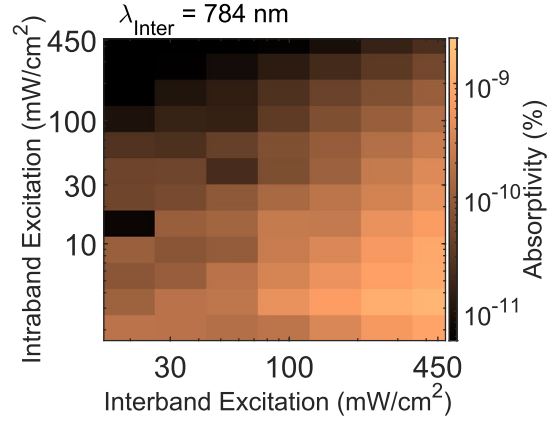


Fig.4 Absorptivity map of the 1319-nm infrared photons as functions of 784-nm interband and 1319-nm intraband excitation power density.

coefficient depends on the excitation intensity. In other words, it depends on the photogenerated electron density. The highest value of the absorption coefficient is  $\sim 5 \times 10^{-5} \text{ cm}^{-1}$ . The calculated absorption coefficient of the TPU process occurring at a heterointerface with QDs was reported with a range between 400–2000  $\text{cm}^{-1}$  [4, 5]. Therefore, this suggests that the TPU process is likely to be achieved by the interface states which are relatively lower in the density of states compared to QDs.

#### 4. Conclusions

We reported the fabrication and fundamental carrier dynamics of quantum-dot-free CsPbBr<sub>3</sub>/GaAs-based TPU-SCs. The TPU process was achieved by the interface states. Although the enhancement of photocurrent can be achieved, it decreases with increasing 1319-nm photon intensity because of the decrease in photoabsorptivity.

#### References

- [1] T. Kita, Y. Harada, and S. Asahi, *Energy Conversion Efficiency of Solar Cells* (Springer Singapore, Singapore, 2019).
- [2] S. Asahi, H. Teranishi, K. Kusaki, T. Kaizu, and T. Kita, *Nat. Commun.* **8**, 1 (2017).
- [3] H. Mahamu, S. Asahi, T. Kita, *J. Appl. Phys.* **133**, 124503 (2023).
- [4] Y. Harada, T. Maeda, T. Kita, *J. Appl. Phys.* **113**, 223511 (2011).
- [5] A. Luque, A. Martí, A. Meller, D. F. Marrón, I. Tonías, E. Antolín, *Prog. Photovolt.* **21**, 658–667 (2013).